Environmental and Molecular Mutagenesis 50:708–717 (2009)

Research Article

Induction of Aneuploidy by Single-Walled Carbon Nanotubes

L.M. Sargent,[1]* A.A. Shvedova,[1,2] A.F. Hubbs,[1] J.L. Salisbury,[3] S.A. Benkovic,[1] M.L. Kashon,[1] D.T. Lowry,[1] A.R. Murray,[1,2] E.R. Kisin,[1] S. Friend,[1] K.T. McKinstry,[1] L. Battelli,[1] and S.H. Reynolds[1]

[1]*National Institute for Occupational Safety and Health, Morgantown, West Virginia*
[2]*West Virginia University, Morgantown, West Virginia*
[3]*Mayo Clinic, Rochester, Minnesota*

Engineered carbon nanotubes are newly emerging manufactured particles with potential applications in electronics, computers, aerospace, and medicine. The low density and small size of these biologically persistent particles makes respiratory exposures to workers likely during the production or use of commercial products. The narrow diameter and great length of single-walled carbon nanotubes (SWCNT) suggest the potential to interact with critical biological structures. To examine the potential of nanotubes to induce genetic damage in normal lung cells, cultured primary and immortalized human airway epithelial cells were exposed to SWCNT or a positive control, vanadium pentoxide. After 24 hr of exposure to either SWCNT or vanadium pentoxide, fragmented centrosomes, multiple mitotic spindle poles, anaphase bridges, and aneuploid chromosome number were observed. Confocal microscopy demonstrated nanotubes within the nucleus that were in association with cellular and mitotic tubulin as well as the chromatin. Our results are the first to report disruption of the mitotic spindle by SWCNT. The nanotube bundles are similar to the size of microtubules that form the mitotic spindle and may be incorporated into the mitotic spindle apparatus. Environ. Mol. Mutagen. 50:708–717, 2009. Published 2009 Wiley-Liss, Inc.†

Key words: spindle; nanoparticles; aneuploidy

INTRODUCTION

Carbon nanotubes are currently used in many consumer and industrial products such as paints, sunscreens, cosmetics, toiletries, electronics, and industrial lubricants. The nanotechnology industry is a multibillion dollar industry and is expected to reach a trillion dollars by 2015. These particles come in two major commercial forms: single-walled carbon nanotubes (SWCNT); and the more rigid, multi-walled carbon nanotubes (MWCNT). The low density and small size of carbon nanotubes makes respiratory exposures likely, with the highest exposures expected to occur occupationally, either during production or their incorporation into various products. Although the industry is expanding rapidly, the associated human health hazards have not been investigated fully.

Although carbon nanotubes can be biodegraded by peroxidases, particularly myeloperoxidase in neutrophils [Allen et al., 2008], they may stay in the body for long periods of time following exposure. The durability, narrow width, and proportionally greater length of these hollow fibers suggest the potential for toxicity similar to asbestos [Muller et al., 2008]. Several studies have demonstrated that SWCNT and MWCNT can enter cells [Monteiro-Riviere et al., 2005; Bottini et al., 2006a,b], and cause a variety of inflammatory, cytotoxic, proliferative, and genetic changes in vitro and in vivo [Shvedova et al., 2005, 2008]. Nanotube exposure induces the

Additional Supporting Information may be found in the online version of this article.

The findings and conclusions in this report are those of the authors and do not necessarily represent the views of the National Institute for Occupational Safety and Health.

Grant sponsor: NIOSH; Grant numbers: OH008282, NORA 927000Y, NORA 9927Z8V; Grant sponsor: 7th Framework Program of the European Commission; Grant number: EC-FP-7-NANOMMUNE-214281.

*Correspondence to: Linda M. Sargent, Toxicology and Molecular Biology Branch, Health Effects Laboratory Division, National Institute for Occupational Safety and Health, 1095 Willowdale Road, Mailstop L-3014, Morgantown, WV 26505, USA. E-mail: lqs1@cdc.gov

Received 16 July 2009; provisionally accepted 6 August 2009; and in final form 7 August 2009

DOI 10.1002/em.20529

Published online 22 September 2009 in Wiley InterScience (www.interscience.wiley.com).

generation of reactive oxygen species, oxidative stress, and cytotoxicity [Lam et al., 2004; Warheit et al., 2004; Risom et al., 2005; Shvedova et al., 2005]. SWCNT appear to interact with the structural elements of the cell, with apparent binding to the cytoskeleton [Porter et al., 2007], telomeric DNA [Li et al., 2006b], and G-C rich DNA sequences in the chromosomes [Li et al., 2006a]. The intercalation of SWCNT into DNA can destabilize the helix, resulting in a conformational change [Li et al., 2006a] that could induce instability and chromosome breakage. Recent studies have shown that in vitro treatment of established cancer cell lines with SWCNT induces DNA damage [Kisin et al., 2007; Pacurari et al., 2008].

SWCNT exposure in mice produces macrophages without nuclei and dividing macrophage daughter cells connected by nanotubes, indicating that SWCNT may be capable of inducing errors in cell division in vivo [Mangum et al., 2006; Shvedova et al., 2008]. Recent studies have demonstrated that the more rigid, larger diameter MWCNT will produce micronuclei in Type II epithelial cells [Muller et al., 2008]. Micronuclei indicate either a high level of chromosomal breakage or mitotic spindle disruption. Exposure of cancer cell lines to MWCNT resulted in the loss of whole chromosomes indicating a possible disruption of the mitotic spindle [Muller et al., 2008]; however, the morphology of the mitotic spindle has not been examined with either MWCNT or SWCNT. The integrity of the mitotic spindle and chromosome number are critical because mitotic spindle disruption, centrosome damage, and aneuploidy may lead to a greater risk of cancer [Aardema et al., 1998; Salisbury et al., 2004]. We, therefore, examined whether exposure to SWCNT had the potential to induce aneuploidy and mitotic spindle aberrations in normal and immortalized human respiratory epithelial cells.

METHODS

Particles for All Experiments

SWCNT (CNI, Houston, TX) produced by the high pressure CO disproportionation process (HiPco) technique, employing CO in a continuous-flow gas phase as the carbon feedstock and $Fe(CO)_5$ as the iron-containing catalyst precursor, and purified by acid treatment to remove metal contaminates were used in this study [Gorelik et al., 2000]. Chemical analysis of total elemental carbon and trace metal (iron) in SWCNT was performed at the Chemical Exposure and Monitoring Branch (DART/NIOSH, Cincinnati, OH). Elemental carbon in SWCNT (HiPco) was assessed according to the NIOSH Manual of Analytical Methods [Birch, 2003], while metal content (iron) was determined using nitric acid dissolution and inductively coupled plasma-atomic emission spectrometry (ICP-AES, NMAM #7300). The purity of HiPco SWCNT was assessed by several standard analytical techniques including thermogravimetric analysis with differential scanning colorimetry (TGA-DSC), thermo-programming oxidation, Raman spectroscopy, and Near-Infrared spectroscopy [Aprepalli, 2004]. The specific surface area was measured at $-196^{\circ}C$ by the nitrogen absorption–desorption technique (Brunauer Emmet Teller method, BET) using a SA3100 Surface Area and Pore Size Analyzer (Beckman Coulter, Fullerton, CA), while diameter and length were measured by transmission electron microscopy. The diameters of purified SWCNT were 1–4 nm. The length of the SWCNT was 0.5–1 μm. Surface area of purified SWCNT was 1,040 m^2/g. The chemical analysis was assessed at DATA CHEM Laboratories using plasma-atomic emission spectrometry. The SWCNT were 99% elemental carbon and 0.23% iron. The same lot of SWCNT was utilized for all experiments reported.

Culture of Cells

Two human respiratory epithelial cell populations were used to examine the potential genetic damage due to SWCNT exposure. Immortalized human bronchial epithelial cell (BEAS-2B) cultures double every 8–10 hr and have normal mitotic spindle morphology (ATCC, Manassas, VA). The proliferation rate and the integrity of the mitotic spindle of the BEAS-2B cells make it possible to examine a minimum of 100 mitotic spindles of good morphology for each of three replicate cultures for each treatment combination. Primary human respiratory epithelial cells (SAEC) isolated from the small airway of a normal human donor were examined to determine the response of a normal cell population to SWCNT exposure. The primary cells have a normal diploid karyotype, which was necessary for the determination of potential aneuploidy induction following exposure. The primary cell cultures double every 20 hr, which makes it possible to analyze a potential change in chromosome number and centrosome morphology following a 24-hr exposure. However, the mitotic index was not sufficient for the analysis of 300 mitotic spindles.

BEAS-2B cells were cultured in DMEM media supplemented with 10% serum, while SAEC were obtained and cultured following manufacturer's directions using Cabrex media (Lonza, Walkersville, MD). Cells of at least 90% purity and 80% viability from a single lot were used for all experiments. Both BEAS-2B and SAEC cell cultures were further examined by electron microscope and cytokeratin 8 and 18 staining to verify the phenotype of the cells.

Treatment Protocol

The immortalized BEAS-2B and the primary SAEC were exposed in parallel culture dishes to SWCNT or to the spindle poison (positive control), vanadium pentoxide. Vanadium pentoxide fragments the centrosome and also inhibits the assembly microtubules resulting in aberrant spindles, aneuploidy, polyploid, and binucleate cells [Ramirez et al., 1997]. The dose of SWCNT was based on previous laboratory exposure levels [Maynard et al., 2004]. SWCNT was suspended in media and then sonicated over ice for 5 min. Vanadium was suspended in media and sonicated over ice in the cold room for 30 min. Specifically, cultured cells were dosed with 24, 48, or 96 $\mu g/cm^2$ SWCNT or to 0.031, 0.31, or 3.1 $\mu g/cm^2$ vanadium pentoxide. Twenty-four hours after exposure all cells were prepared for analysis of apoptosis and necrosis, integrity of the mitotic spindle, as well as the centrosome and chromosome number. Three independent replicates were performed for each exposure of the SAEC and BEAS-2B.

Viability and Apoptosis

Triplicate cultures were prepared in 96-well plates for the analysis of viability using the Alamar Blue bioassay (Invitrogen, Carlsbad, CA), following procedures described previously [Keane et al., 1997]. Parallel cultures were also prepared in duplicate in 1-ml chamber slides for the analysis of apoptosis using the TUNEL assay following the manufacturer's directions (Roche, Indianapolis, IN) with some modifications outlined previously [Gavrieli et al., 1992]. An additional positive control slide was treated with 400 Kunitz units DNase1 (D4263, Sigma-Aldrich, Saint Louis, MO). The DNase 1 fragments the DNA to simulate the

fragmentation of the chromatin that occurs during apoptosis. The exposed 3-0H DNA ends are labeled with fluorescein-12-dUTP. Twenty-four hours after dosing, the cells were fixed in 4% paraformaldehyde in PBS, pH 7.4, stained with DAPI and fluorescein, and photographed using a Zeiss Axiophot fluorescent microscope. A minimum of 50 cells were analyzed for each culture chamber for a total of 100 cells, which was repeated three times for a total of 300 cells for each treatment and dose.

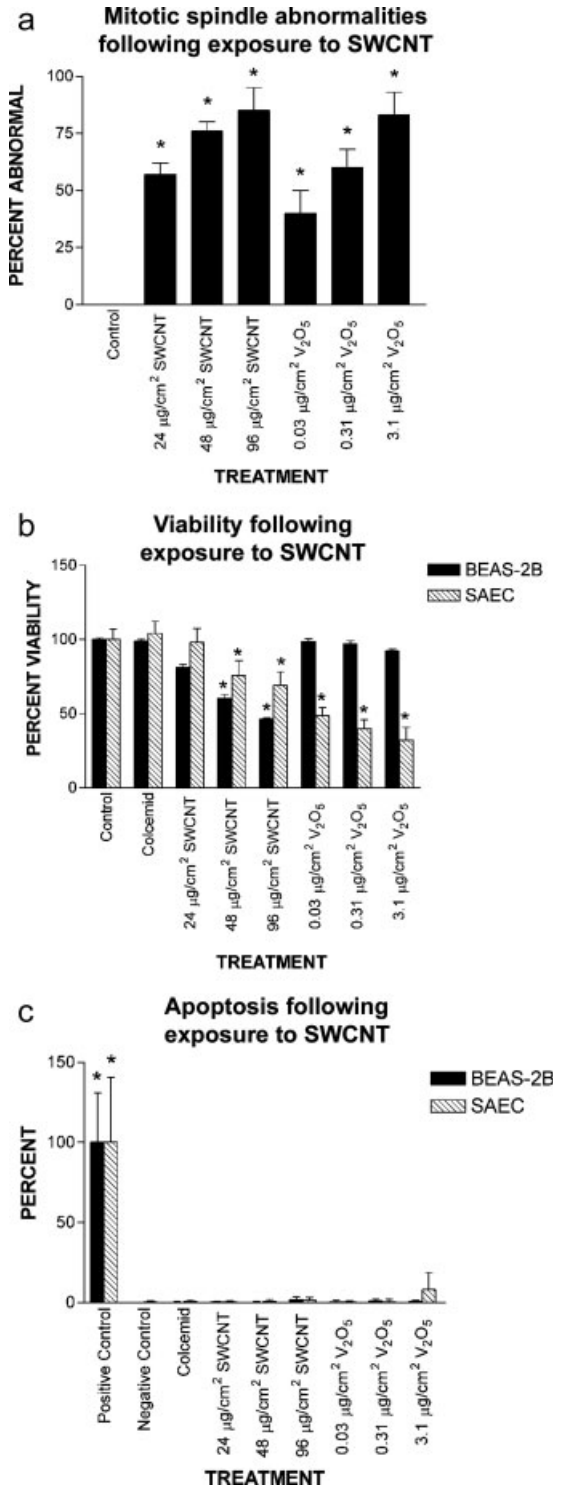

Mitotic Spindle and Centrosome Morphology Analysis

BEAS-2B and SAEC were cultured in 1-ml chamber slides. Dual chambers were prepared for each treatment and cell type. Three independent replicates were prepared for each cell type and treatment. Spindle integrity and centrosome number were examined using dual-label immunofluorescence for tubulin and centrin to detect the mitotic spindle and the centrosomes, respectively. Primary antibodies were rabbit anti-β tubulin (Abcam, La Jolla, CA) and mouse anti-centrin (a generous gift from Dr. Jeff Salisbury) and secondary antibodies were Rhodamine Red goat anti-rabbit IgG and Alexa 488 goat anti-mouse IgG (Invitrogen). Aggregated SWCNT (carbon nanoropes) could be visualized by their interference with transmitted light using differential interference contrast (DIC) imaging. Morphology of the mitotic spindle and centrosome, and the relationship with carbon nanoropes, were analyzed in the BEAS-2B cells using a laser scanning confocal microscope (LSM 510, Carl Zeiss MicroImaging, Thornwood, NY) as previously described [Salisbury et al., 2004]. To localize carbon nanoropes to the microtubules of the mitotic spindle and the centrosome, serial optical slices were obtained to create a z-stack and permit three-dimensional reconstruction using LightWave software [Haas and Fischer, 1997]. At least 50 cells per chamber and a total of 300 cells of good centrosome and 300 cells of good mitotic spindle morphology were analyzed for each treatment dose for BEAS-2B. The centrosome morphology was analyzed in 300 cells for each dose and treatment in the SAEC cultures. Transmission electron microscopy was used to examine centrosome integrity as previously described [Salisbury et al., 2004].

Chromosome Number by FISH

The bar graph indicates the chromosome loss and gain that was observed in BEAS-2B and SAEC following exposure to SWCNT and V_2O_5. Aneuploidy was determined using fluorescent in situ hybridization (FISH) for human chromosomes 1 and 4 (Abott Molecular, Des Plaines, IL). The chromosome number was determined following the guidelines of the American College of Medical Genetics [Genetics, 2006]. The chromosome number was estimated by counting the number of signals for chromosomes 1 and 4 in a minimum of 100 interphase cells of good FISH morphology. The cells were photographed using a Zeiss Axiophot microscope and Applied Imaging software. The experiment was repeated three times for a total of three independent replications and 300 evaluated cells per treatment and dose.

Fig. 1. Toxicity of SWCNT. (**a**) Figure 1 shows the percentage of cells that were observed with mitotic spindle abnormalities. The solid bars indicate the level of apoptosis in control and exposed BEAS-2B. Mitotic spindle abnormalities are expressed as a percent of total mitotic figures. The abnormalities included monopolar, tripolar, and quadrapolar mitotic spindles, and nanotubes displacing portions of the mitotic spindle. * indicates significantly different from the unexposed control cells at $P < 0.001$. (**b**) The bar graph shows viability of BEAS-2B and SAEC cells following exposure to SWCNT or V_2O_5. The solid bars indicate the level of viability in control and exposed BEAS-2B. The hatched bars indicate the level of apoptosis in the exposed SAEC. SWCNT exposure resulted in reduced viability in the Alamar Blue assay in the SAEC and the BEAS-2B at 48 and 96 μg/cm^2 compared to control cells. The exposure to V_2O_5 resulted in reduced viability in SAEC-treated cells at all doses; however, a reduction in viability was not observed in the V_2O_5-treated BEAS-2B cells. *Indicates statistical significance at $P < 0.001$. (**c**) The solid bars indicate the percentage of apoptotic cells in control and exposed BEAS-2B. The hatched bars indicate the percentage of apoptotic cells in control and exposed SAEC. The DNase-treated positive control showed significant apoptosis in the BEAS-2B and the SAEC; however, exposure to SWCNT or V_2O_5 did not induce apoptosis.

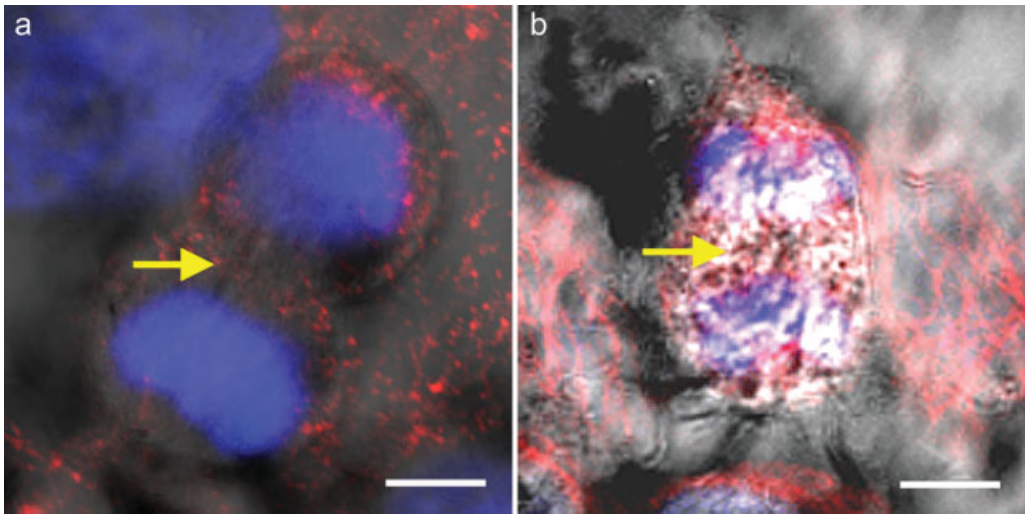

Fig. 2. SWCNT-induced disruption of anaphase. (**a** and **b**) A composite of two SWCNT-treated cells treated on separate days. The DNA in (a) and (b) were detected by DAPI and were blue. The tubulin in (a) and (b) were stained red using Spectrum red and indirect immunofluorescence. The nanotubes in (a) and (b) were imaged using differential interference contrast. The mitotic cells are in the anaphase stage of cell division when the DNA is separating into daughter cells. The nanotubes indicated by yellow arrows are in the bridge of the separating daughter cells (bridge of cytokinesis or midbody).

Statistical Analysis

The mean and the standard deviation were determined by the analysis of duplicate samples in three separate experiments. Chi-square analysis was used to determine statistical significance for the scoring of the mitotic spindle abnormalities, the number of cells with damaged centrosomes, the number of viable cells, the number of apoptotic cells, and the number of cells with abnormal chromosome number. A significance of $P < 0.01$ was considered significant.

RESULTS

Two human bronchial epithelial cell populations were used to examine the potential of SWCNT to induce genetic damage. Because of the necessity of a normal diploid karyotype, primary small airway epithelial cells (SAEC, Lonza) were used to examine chromosome number. Immortalized respiratory epithelial cells were also included in the study of centrosome and mitotic spindle integrity, viability, and apoptosis. Treatment with SWCNT induced a large increase in the frequency of monopolar, tripolar, and quadrapolar mitotic spindles in both normal and immortalized human respiratory epithelial cells. This increase was similar to the pattern observed in the vanadium pentoxide-treated cells (Fig. 1a). Cell viability was significantly reduced in primary respiratory epithelial cells (SAEC) following treatment with the medium or high concentration of SWCNT, and all three concentrations of vanadium pentoxide. Similarly, with respect to the SWCNT treatment, immortalized bronchial epithelial cells (BEAS-2B) showed a reduction in cell viability following treatment with the medium or high concentration of SWCNT; however, treatment with vanadium pentoxide did not reduce cell viability in these cells (Fig. 1b). This reduced viability was not due to the induction of apoptotic pathways as neither SWCNT nor vanadium pentoxide resulted in detectable apoptosis (Fig. 1c).

SWCNT form bundles in aqueous environments due to their highly hydrophobic surfaces. Although a single carbon nanotube (1–4 nm) can not be imaged, small bundles of nanotubes of 10 nm or greater can be observed using DIC imaging. SWCNT were observed in the midbody or bridge separating dividing cells (Fig. 2). Multipolar mitotic spindles were observed with nanotubes in the nucleus (Figs. 3a–3d). Physical associations were observed between SWCNT and the DNA, as well as the microtubules of the mitotic spindle (Figs. 4a–4d). Specifically, following administration of the high dose of SWCNT, distortion of the mitotic spindle was observed in 15% of treated cells (Figs. 4a–4d). The location of the nanotubes was confirmed by serial optical images of 0.1 μm (Supporting Information Fig. 1). Anaphase bridges or lagging chromosomes were seen in 8% of cells (Fig. 4e), and nanotubes were observed in 15% of the bridge of cytokinesis between dividing cells.

The centrosome determines the shape of the mitotic spindle and the cytoskeleton [Salisbury, 2008], and abnormal spindle morphology will result in unequal distribution of the chromosomes. Centrosome morphology and number can be determined in both interphase and mitotic cells, making it possible to examine part of the mitotic spindle in the primary respiratory epithelial cells. The centrosome morphology of the untreated BEAS-2B and/or SAEC was 1–2 centrosomes/cell as expected (Fig. 5a).

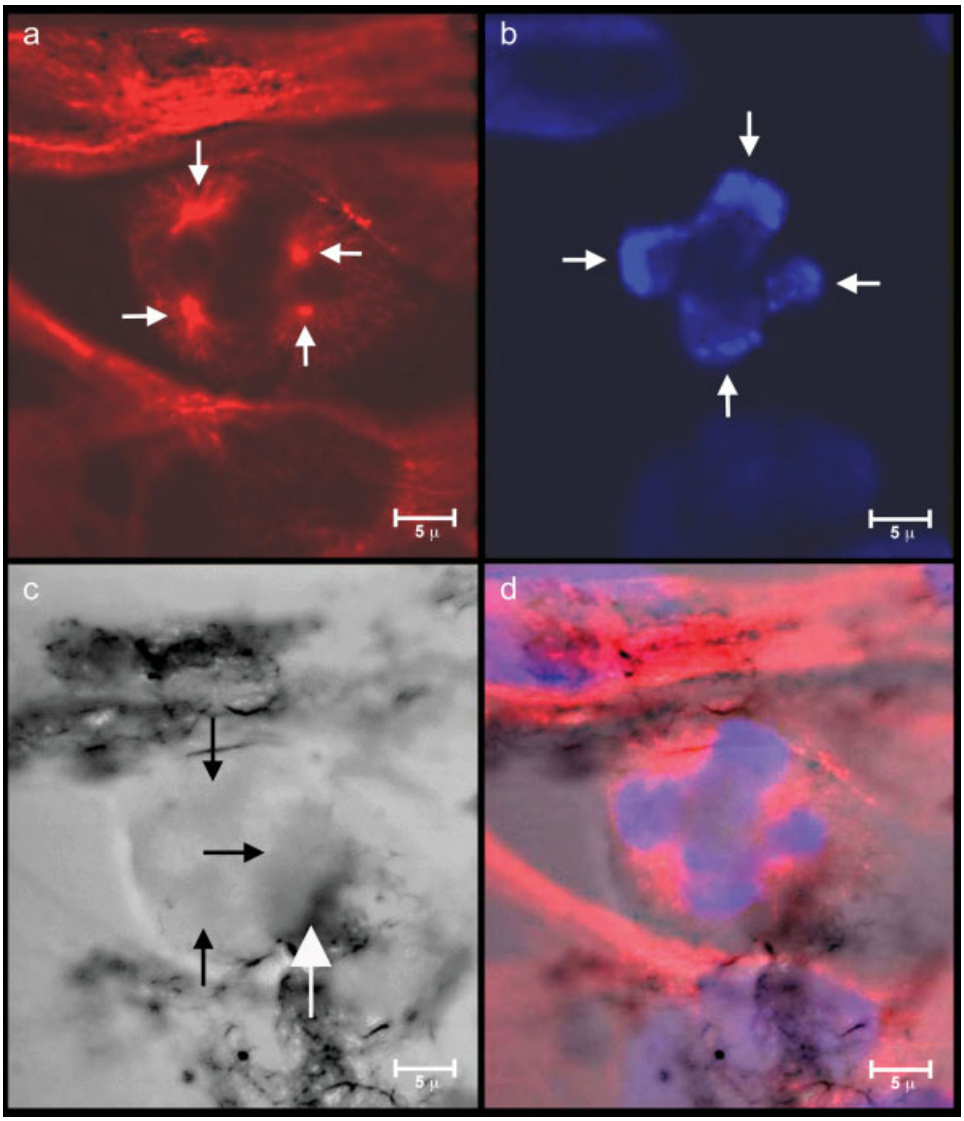

Fig. 3. SWCNT-treated cell with four spindle poles. The photographs in (**a**–**d**) show a multipolar mitotic spindle with four poles rather than the two poles that would be expected in a normal cell. The details of the detection protocol for the mitotic spindle components and the photography using the Zeiss Confocal are in the methods. The tubulin in (a) was stained red using Spectrum red and indirect immunofluorescence. White arrows in (a) indicate the four mitotic spindle poles. The DNA in (b) was detected by DAPI and was blue. The DNA is being pulled four ways as indicated by white arrows. The nanotubes in (c) were imaged using differential interference contrast. The nanotubes can be seen in the nucleus. The SWCNT vary from dense black areas of tightly packed nanoropes indicated by a large white arrow to lighter areas containing only a few loosely arranged nanoropes indicated by small black arrows. The composite image in (d) shows the merged image of the DNA, tubulin, and nanotubes images. Serial optical sections at 0.1-μm intervals using confocal microscopy confirmed the location of the nanotubes in the nuclear DNA and the tubulin including the microtubules of the mitotic spindle.

BEAS-2B treated with SWCNT demonstrated a dose–response of fragmentation of the centrosome at levels higher than the positive control, vanadium pentoxide (Fig. 5a). The integrity of the centrosome was confirmed by Transmission Electron Microscopy (data not shown). When the SWCNT-treated normal SAEC were examined, the dose–response of centrosome fragmentation was comparable to the damage observed in the SWCNT-treated BEAS-2B cells (Figs. 5b–5e). DIC imaging showed that the nanotubes were in association with the centrosome (Figs. 5b–5e). Z-stack imaging of 0.1-μm sections confirmed the association of the nanotubes with the centrosome (Supporting Information Fig. 2). The optical sections were used to construct a 3D image. The 3D image shows the association of SWCNT with the centrosomes that occurred at all doses utilized in the current study.

The chromosome number was analyzed in the primary SAEC from a normal donor. The SAEC were used to

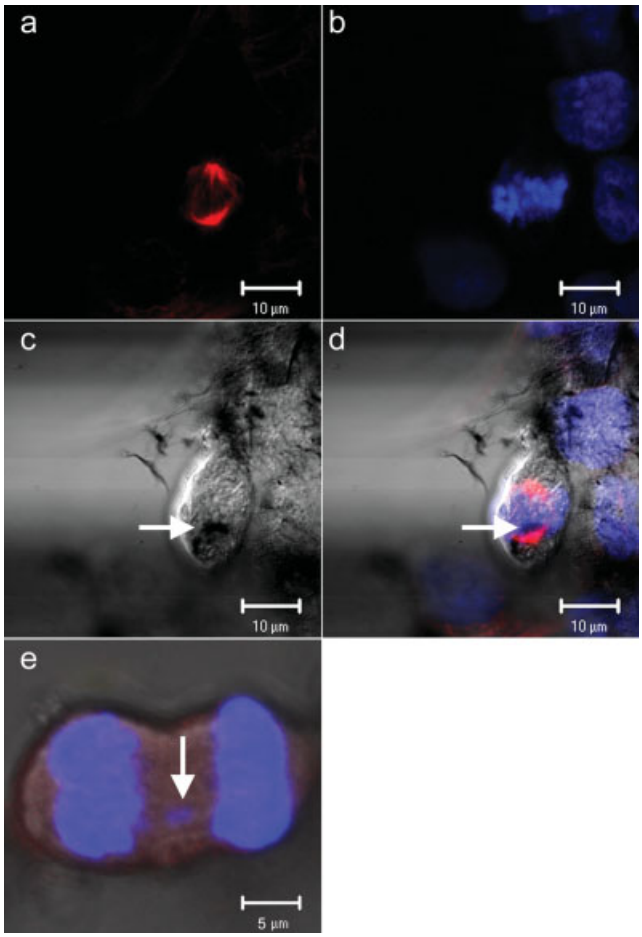

Fig. 4. Nanotubes displace DNA in SWCNT-treated cells when viewed by confocal immunofluorescent and DIC microscopy. (**a**) Spindle disruption by SWCNT is demonstrated using indirect immunofluorescence to stain tubulin red and reveal the microtubules. (**b**) DNA stains blue using DAPI. (**c**) The SWCNT are black when viewed using DIC (arrow). (**d**) The composite image shows intimate association between SWCNT and DNA and SWCNT and tubulin in this 0.1-μm optical section. The SWCNT above the lower spindle pole (arrow) appears to displace the microtubules that normally radiate from the spindle pole. (**e**) In this combined DAPI and DIC image of a different mitotic figure, a DNA fragment has broken off (arrow) as the duplicated DNA separates in anaphase forming an anaphase bridge.

assure a normal karyotype for the accurate evaluation of treatment-associated aneuploidy. FISH analysis for chromosome 1 or 4 revealed approximately in (5 ± 2)% aneuploidy in control primary respiratory cells (Fig. 6). The frequency of the aneuploid cells in the controls is within the range reported in adult human cells in culture [Yurov et al., 2005; Wiktor et al., 2006]. In contrast, the SWCNT-treated SAEC had a level of aneuploidy that was as high as the effect that was observed in the vanadium pentoxide-treated positive control cells (Fig. 6). SWCNT-induced aneuploidy was increased to 50% at the lowest concentration of 24 μg/cm^2 and 77% at the highest concentration of 96 μg/cm^2 (Fig. 6).

DISCUSSION

Our data are the first to show that orderly cell division was frequently disrupted by SWCNT. Exposure to 24 μg/cm^2 SWCNT or higher resulted in chromosomal aneuploidy and mitotic spindle aberrations in greater than 50% of the cells examined. The level of centrosome fragmentation, mitotic spindle damage, and aneuploidy following SWCNT exposure was similar to the effects of the known carcinogen and positive control, vanadium pentoxide. Furthermore, the SWCNT were found in association with the centrosome clusters. Specifically, nanotubes were observed attached to the centrosomes forming a spindle-like structure that seemed to pull the DNA toward the centrosome. Fragmentation of the centrosome can be induced by global DNA damage [Hut et al., 2003], inhibition of mitotic spindle motor movement or activity [Abal et al., 2005; Krzysiak et al., 2006], or by inhibiting the processing of misfolded centrosome proteins [Ehrhardt and Sluder, 2005]. Although the 8% increased level of DNA breakage in the high-dose SWCNT-exposed group is significant as estimated by the anaphase bridges, the damage is not sufficient to explain centrosome damage in 80% of the cells. The positive control, vanadium pentoxide is believed to induce centrosome fragmentation, mitotic spindle disruption, and aneuploidy through the inhibition of the spindle motor dynein [Evans et al., 1986; Ramirez et al., 1997; Ma et al., 1999]. Previous work indicated that spherical nanoparticles of 40 nm or less could inhibit the mitotic spindle motor kinesin that is essential for normal cell division [Bachand et al., 2005]. The confocal microscopy studies described in this manuscript suggest direct interaction with the centrosomes. This interaction may be due to the incorporation of SWCNT into cellular structures similar to the incorporation that has been observed in bone [Aoki et al., 2007]. Indeed, the diameter of SWCNT nanoropes is comparable to the size of cellular and mitotic microtubules, suggesting that SWCNT may displace tubulin at critical cellular targets. Physical interaction with the mitotic apparatus and multipolar spindles have been observed following chrysotile asbestos exposure [Cortez and Machado-Santelli, 2008]. Disruption of the mitotic spindle is highly associated with carcinogenesis.

In vitro studies provide insight into the potential toxicity of SWCNT. Nanotubes appear to interact with the structural elements of the cell, with apparent binding to the cytoskeleton [Porter et al., 2007], as well as binding to telomeric DNA [Li et al., 2006b]. In addition, SWCNT also bind to G-C rich DNA sequences in the chromosomes [Li et al., 2006a]. The intercalation of SWCNT could destabilize DNA resulting in a conformational change [Li et al., 2006a,b]. Intercalating agents can also induce chromosome breakage and instability. Previous

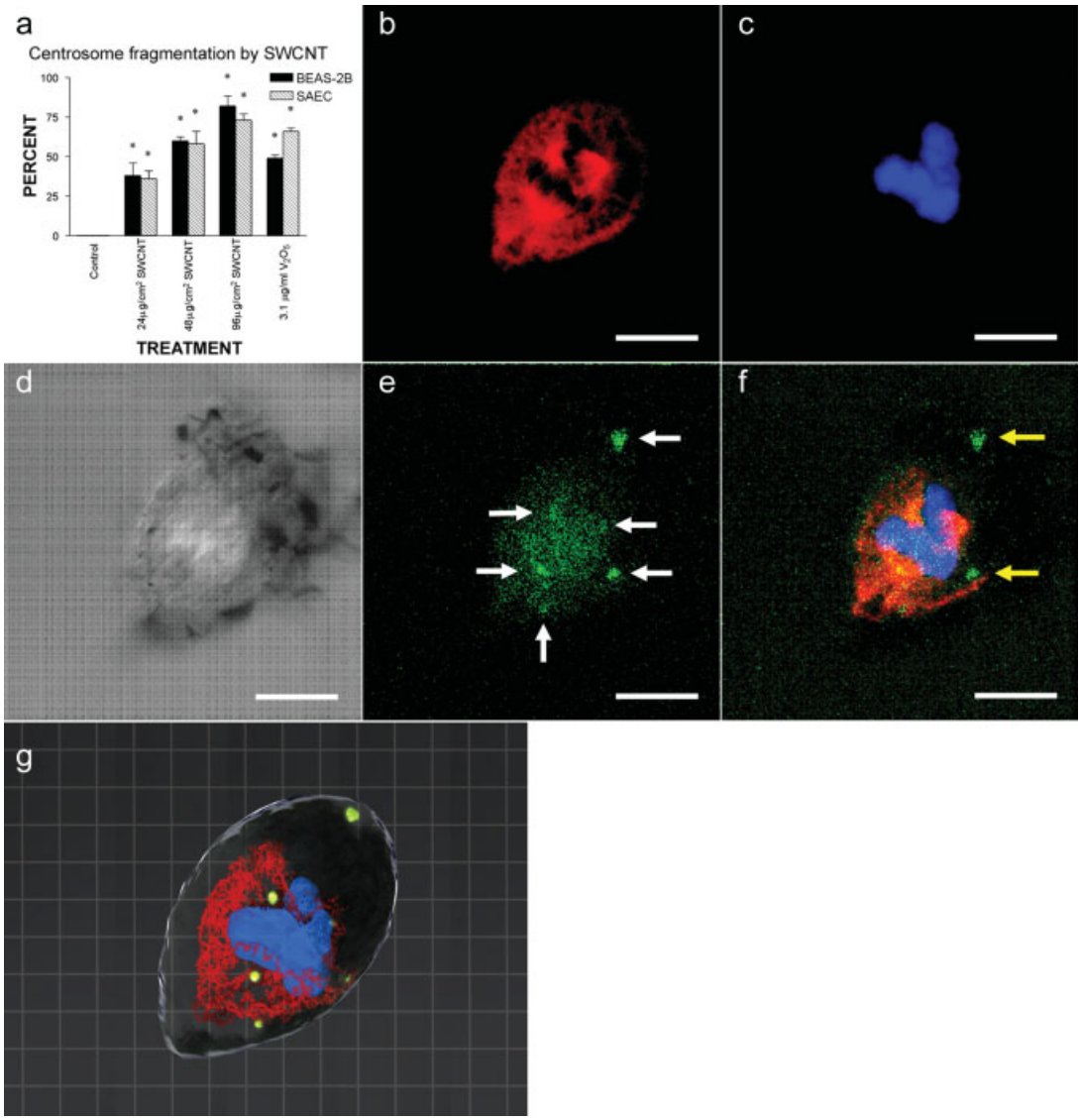

Fig. 5. Centrosome damage following SWCNT exposure. (**a**) The bar graph demonstrates the percent of BEAS-2B and SAEC with centrosome fragmentation 24 hr after exposure to the positive control vanadium pentoxide (V_2O_5) or to SWCNT. SWCNT exposure increased centrosome fragmentation in both BEAS-2B and SAEC at all doses of exposure at levels comparable to the positive control V_2O_5. * indicates significantly different from the unexposed control cells at $P < 0.001$. (**b**) The figure in (**b–d**) is a multipolar mitotic spindle with three poles rather than the two poles that would be expected in a normal cell. The tubulin in (b) was stained red using Spectrum red by indirect immunofluorescence. The DNA in (c) was detected by DAPI and was blue. The nanotubes in (d) were imaged using differential interference contrast and are black. The centrosomes in (**e**) were detected using Alexa 488 (Invitrogen) and are green. The centrosomes in (e) are indicated by white arrows. In (**f**) the DNA, tubulin, nanotubes, and centrosome images were merged. The yellow arrows in (f) indicate centrosomes that were in association with nanotubes. In (**g**), optical sections of 0.1 μm were used to construct a 3D image of the tripolar mitosis. The reconstructed image shows nanotubes inside the cell in association with the centrosomes, the microtubules, and the DNA. The nanotubes in (b–g) appear to be pulling the DNA in a manner similar to that observed by the mitotic spindle tubulin. Since SWCNT associate with DNA and centrosomes and displace the tubulin of the mitotic spindle, they appear to pull the DNA toward the spindle poles. In this cell, the three spindle poles, the three unequal DNA bundles, and the disruption of microtubule attachments to two centrosomes suggest major perturbations in cell division.

investigations have shown that in vitro treatment of established cancer cell lines with 96, 48, and 24 μg/cm^2 SWCNT induces DNA damage as measured by the comet assay [Kisin et al., 2007]. More recent studies have demonstrated that MWCNT will induce micronuclei in Type II epithelial cells 3 days following dosing with 1 mg/kg MWCNT [Muller et al., 2008] and SWCNT exposure results in macrophages without a nucleus [Shvedova et al., 2008]. Micronuclei and cells without nuclei indicate possible mitotic spindle disruption. Exposure of cancer

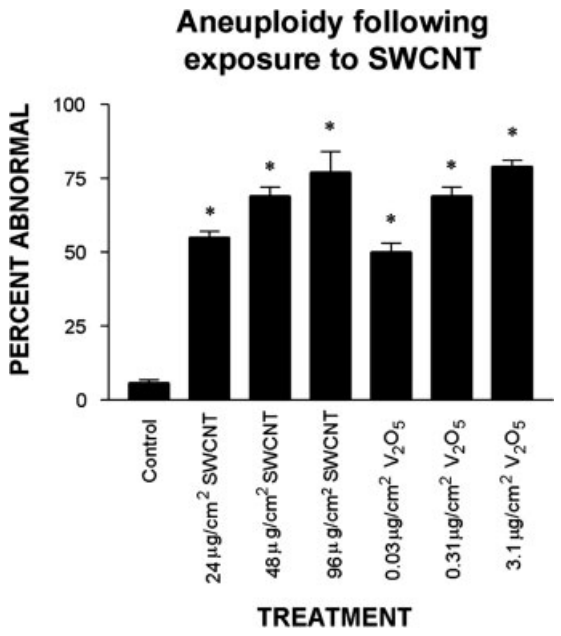

Fig. 6. Aneuploidy in primary human respiratory epithelial cell cultures following exposure to SWCNT: The bar graph demonstrates the percent of SAEC with an aneuploid chromosome number after a 24-hr exposure to SWCNT or the positive control V_2O_5. The solid bars indicate the level of apoptosis in the exposed and control BEAS-2B. The hatched bars indicate the level of apoptosis in the exposed SAEC. SWCNT exposure induced a dramatic elevation of chromosome loss and gain at all doses of exposure at levels equal to the positive control V_2O_5. *Indicates significantly different from the unexposed control cells at $P < 0.001$.

cell lines to MWCNT demonstrated the loss of whole chromosomes further indicating a disruption of the mitotic spindle [Muller et al., 2008]; however, the morphology of the mitotic spindle has not been previously examined.

Results from in vivo exposure to SWCNT have demonstrated mutations in K-ras [Shvedova et al., 2008], indicating that SWCNT may be capable of inducing DNA damage in vivo. The observation of mutations of the K-ras oncogene in SWCNT-exposed mouse lungs [Shvedova et al., 2008] indicates genotoxicity and the potential to initiate lung cancer. Mutations of the K-ras gene are frequently reported in chemically-induced mouse lung tumors and smoking-induced human lung adenocarcinoma [Pao et al., 2004; Tam et al., 2006; Chan et al., 2007; Hong et al., 2007]. Persistent epithelial proliferation is a feature of the second phase of pulmonary carcinogenesis (promotion) [Pitot et al., 1989; Pitot, 1996, 2007; Rubin, 2001]. Given that epithelial hyperplasia and cellular atypia were noted in mice exposed to SWCNT in vivo [Shvedova et al., 2008], the potential for carcinogenicity is particularly concerning. Recent investigations of multi-walled-carbon-nanotubes (MWCNT) carcinogenicity have demonstrated that injection of high doses of nanotubes results in mesotheliomas in p53 ± transgenic mice and in rats [Takagi et al., 2008; Sakamoto et al., 2009]. Although the MWCNT exposure studies have been criticized due to the high dose and the route of exposure, the studies raise concerns about the potential of cancer due to occupational and environmental exposures to particles that may have physical properties similar to asbestos fibers.

The extraordinary level of chromosomal abnormalities following SWCNT exposure underscores the importance of the SWCNT-induced damage to the mitotic spindle, and the importance of additional studies to uncover the mechanism of damage. Mitotic spindle damage and aneuploidy have also been observed following in vitro treatment with 0.25 mg/ml of the potent occupational carcinogen, chrysotile asbestos [Cortez and Machado-Santelli, 2008]. The dose of the chrysotile used in the in vitro studies was 10-fold higher than the lowest dose of SWCNT that induced similar damage. The diameter and length of the asbestos fibers have been shown to be critical for the interaction with the mitotic spindle and for the induction of cancer. Fibers with a diameter of less than 0.5 μm and a length of 5–30 μm have been shown to induce mitotic spindle damage and mesotheliomas [Harington, 1981; Stanton et al., 1981; Cortez and Machado-Santelli, 2008]. Chrysotile asbestos has been observed in DNA and in the bridge of cytokinesis; however, association with the centrosome, centrosome damage, or integration with the mitotic spindle has not been documented following asbestos exposure. SWCNT-treated cells did not die through apoptosis and had a low level of necrosis after 24 hr of exposure, indicating a greater probability of passing genetic damage to daughter cells. A similar low level of toxicity and apoptosis as well as incorporation into cellular structures have been observed in SWCNT-exposed osteoblasts, macrophages, and leukemia cells [Cherukuri et al., 2004; Zanello et al., 2006; Aoki et al., 2007]. Further research is in progress to examine the mechanism and persistence of mitotic spindle damage as well as the potential of delayed cell death following chronic exposure.

More than 25 years ago, Mearl Stanton, in his final publication, considered the potential mechanism of carcinogenesis for the classic carcinogenic fiber, amphibole asbestos, and noted ''A provocative explanation relates to the ability of fine, long fibers to penetrate cells without killing them [Stanton et al., 1981]''. Our results suggest that SWCNT may indeed exert genotoxic effects due to their resistance to biological clearance, in addition to specific interactions with cellular components that alters the orderly progression of cell division. The nanotube bundles are similar to the size of the microtubules [Mercer et al., 2008], and may be incorporated into the mitotic spindle rather than the physical interference of the spindle that occurs with the larger asbestos fibers [Cortez and Machado-Santelli, 2008]. Centrosome fragmentation, mitotic spindle disruption, and aneuploidy are characteristics

of cancer cells and may lead to an increased risk of cancer [Aardema et al., 1998; Salisbury et al., 2004]. Long-term in vitro and in vivo studies are required to evaluate whether pulmonary exposure to SWCNT would result in lung cancer.

ACKNOWLEDGMENTS

The authors thank Kimberly Clough-Thomas, NIOSH Morgantown WV for her help with the figures. They thank Mike Gipple, Morgantown WV for his help with the images. They also thank Dr. Robert Mercer, NIOSH Morgantown WV for his consultation on the imaging of nanotubes.

REFERENCES

Aardema MJ, Albertini S, Arni P, Henderson LM, Kirsch-Volders M, Mackay JM, Sarrif AM, Stringer DA, Taalman RD. 1998. Aneuploidy: A report of an ECETOC task force. Mutat Res 410:3–79.

Abal M, Keryer G, Bornens M. 2005. Centrioles resist forces applied on centrosomes during G2/M transition. Biol Cell 97:425–434.

Allen BL, Kichambare PD, Gou P, Vlasova II, Kapralov AA, Konduru N, Kagan VE, Star A. 2008. Biodegradation of single-walled carbon nanotubes through enzymatic catalysis. Nano Lett 8:3899–3903.

Aoki N, Akasaka T, Watari F, Yokoyama A. 2007. Carbon nanotubes as scaffolds for cell culture and effect on cellular functions. Dent Mater J 26:178–185.

Aprepalli S. 2004. Protocol for the characterization of single walled carbon nanotubes. Carbon 1:51–66.

Bachand M, Trent AM, Bunker BC, Bachand GD. 2005. Physical factors affecting kinesin-based transport of synthetic nanoparticle cargo. J Nanosci Nanotechnol 5:718–722.

Birch ME. 2003. Elemental carbon. Monitoring of diesel exhaust particulate in the workplace. In: NIOSH Manual of analytical Methods (NMAM 5040) 4th ed. DHHS publication no. 2003-154), Eds. Cassienelli ME, O'Conner PF. Cincinnati, OH: DHHS publication no. 2003-154), 229–259.

Bottini M, Balasubramanian C, Dawson MI, Bergamaschi A, Bellucci S, Mustelin T. 2006a. Isolation and characterization of fluorescent nanoparticles from pristine and oxidized electric arc-produced single-walled carbon nanotubes. J Phys Chem B Condens Matter Mater Surf Interfaces Biophys 110:831–836.

Bottini M, Bruckner S, Nika K, Bottini N, Bellucci S, Magrini A, Bergamaschi A, Mustelin T. 2006b. Multi-walled carbon nanotubes induce T lymphocyte apoptosis. Toxicol Lett 160:121–126.

Chan PC PJ, Bristol DW, Bucher JR, Burka LT, Chahabra RS, Herbert RA, ing-Herbert AP, Kissling DE, Malarkey DF, Peddada SD, Roycroft JH, Smith CS, Travlos GS, Witt KL, Sills RC. 2007. Toxicology and carcinogenesis studies of cumene in F344/N rats and B6C3F1 mice (inhalation studies). National Toxicology Program. NIH Publication No. 07-5885. pp 1–104.

Cherukuri P, Bachilo SM, Litovsky SH, Weisman RB. 2004. Near-infrared fluorescence microscopy of single-walled carbon nanotubes in phagocytic cells. J Am Chem Soc 126:15638–15639.

Cortez BA, Machado-Santelli GM. 2008. Chrysotile effects on human lung cell carcinoma in culture: 3-D reconstruction and DNA quantification by image analysis. BMC Cancer 8:181.

Ehrhardt AG, Sluder G. 2005. Spindle pole fragmentation due to proteasome inhibition. J Cell Physiol 204:808–818.

Evans JA, Mocz G, Gibbons IR. 1986. Activation of dynein 1 adenosine triphosphatase by monovalent salts and inhibition by vanadate. J Biol Chem 261:14039–14043.

Gavrieli Y, Sherman Y, Ben-Sasson SA. 1992. Identification of programmed cell death in situ via specific labeling of nuclear DNA fragmentation. J Cell Biol 119:493–501.

Genetics ACoM. 2006. Standards and Guidelines for Clinical Genetics Laboratories. Documentation of FISH resutls. 2006 ed. Bethesda, MD. Available at http://www.acmg.net/Pages/ACMG_Activities/stds-2002/stdsmenu-n.htm.

Gorelik O, Nikolaev P, Arepalli S. 2000. Purification Procedures for Single-Walled Carbon Nanotubes. Hanover, MD: NASA Contractor Report.

Haas A, Fischer MS. 1997. Three-dimensional reconstruction of histological sections using modern product-design software. Anat Rec 249:510–516.

Harington JS. 1981. Fiber carcinogenesis: Epidemiologic observations and the Stanton hypothesis. J Natl Cancer Inst 67:977–989.

Hong HH, Dunnick J, Herbert R, Devereux TR, Kim Y, Sills RC. 2007. Genetic alterations in K-ras and p53 cancer genes in lung neoplasms from Swiss (CD-1) male mice exposed transplacentally to AZT. Environ Mol Mutagen 48:299–306.

Hut HM, Lemstra W, Blaauw EH, Van Cappellen GW, Kampinga HH, Sibon OC. 2003. Centrosomes split in the presence of impaired DNA integrity during mitosis. Mol Biol Cell 14:1993–2004.

Keane RW, Srinivasan A, Foster LM, Testa MP, Ord T, Nonner D, Wang HG, Reed JC, Bredesen DE, Kayalar C. 1997. Activation of CPP32 during apoptosis of neurons and astrocytes. J Neurosci Res 48:168–180.

Kisin ER, Murray AR, Keane MJ, Shi XC, Schwegler-Berry D, Gorelik O, Arepalli S, Castranova V, Wallace WE, Kagan VE, Shvedova AA. 2007. Single-walled carbon nanotubes: Geno- and cytotoxic effects in lung fibroblast V79 cells. J Toxicol Environ Health A 70:2071–2079.

Krzysiak TC, Wendt T, Sproul LR, Tittmann P, Gross H, Gilbert SP, Hoenger A. 2006. A structural model for monastrol inhibition of dimeric kinesin Eg5. EMBO J 25:2263–2273.

Lam CW, James JT, McCluskey R, Hunter RL. 2004. Pulmonary toxicity of single-wall carbon nanotubes in mice 7 and 90 days after intratracheal instillation. Toxicol Sci 77:126–134.

Li X, Peng Y, Qu X. 2006a. Carbon nanotubes selective destabilization of duplex and triplex DNA, inducing B-A transition in solution. Nucleic Acids Res 34:3670–3676.

Li X, Peng Y, Ren J, Qu X. 2006b. Carboxyl-modified single-walled carbon nanotubes selectively induce human telomeric i-motif formation. Proc Natl Acad Sci USA 103:19658–19663.

Ma S, Trivinos-Lagos L, Graf R, Chisholm RL. 1999. Dynein intermediate chain mediated dynein-dynactin interaction is required for interphase microtubule organization and centrosome replication and separation in Dictyostelium. J Cell Biol 147:1261–1274.

Mangum JB, Turpin EA, Antao-Menezes A, Cesta MF, Bermudez E, Bonner JC. 2006. Single-walled carbon nanotube (SWCNT)-induced interstitial fibrosis in the lungs of rats is associated with increased levels of PDGF mRNA and the formation of unique intercellular carbon structures that bridge alveolar macrophages in situ. Part Fibre Toxicol 3:15.

Maynard AD, Baron PA, Foley M, Shvedova AA, Kisin ER, Castranova V. 2004. Exposure to carbon nanotube material: Aerosol release during the handling of unrefined single-walled carbon nanotube material. J Toxicol Environ Health A 67:87–107.

Mercer RR, Scabilloni J, Wang L, Kisin E, Murray AR, Schwegler-Berry D, Shvedova AA, Castranova V. 2008. Alteration of deposition pattern and pulmonary response as a result of improved dispersion of aspirated single-walled carbon nanotubes in a mouse model. Am J Physiol Lung Cell Mol Physiol 294:L87–L97.

Monteiro-Riviere NA, Nemanich RJ, Inman AO, Wang YY, Riviere JE. 2005. Multi-walled carbon nanotube interactions with human epidermal keratinocytes. Toxicol Lett 155:377–384.

Muller J, Decordier I, Hoet PH, Lombaert N, Thomassen L, Huaux F, Lison D, Kirsch-Volders M. 2008. Clastogenic and aneugenic effects of multi-wall carbon nanotubes in epithelial cells. Carcinogenesis 29:427–433.

Pacurari M, Yin XJ, Zhao J, Ding M, Leonard SS, Schwegler-Berry D, Ducatman BS, Sbarra D, Hoover MD, Castranova V, Vallyathan V. 2008. Raw single-wall carbon nanotubes induce oxidative stress and activate MAPKs, AP-1, NF-κB, and Akt in normal and malignant human mesothelial cells. Environ Health Perspect 116:1211–1217.

Pao W, Miller V, Zakowski M, Doherty J, Politi K, Sarkaria I, Singh B, Heelan R, Rusch V, Fulton L, Mardis E, Kupfer D, Wilson R, Kris M, Varmus H. 2004. EGF receptor gene mutations are common in lung cancers from ''never smokers'' and are associated with sensitivity of tumors to gefitinib and erlotinib. Proc Natl Acad Sci USA 101:13306–13311.

Pitot HC. 1996. Stage-specific gene expression during hepatocarcinogenesis in the rat. J Cancer Res Clin Oncol 122:257–265.

Pitot HC. 2007. Adventures in hepatocarcinogenesis. Annu Rev Pathol 2:1–29.

Pitot HC, Campbell HA, Maronpot R, Bawa N, Rizvi TA, Xu YH, Sargent L, Dragan Y, Pyron M. 1989. Critical parameters in the quantitation of the stages of initiation, promotion, and progression in one model of hepatocarcinogenesis in the rat. Toxicol Pathol 17 (4 Part 1):594–611; discussion 611–612.

Porter AE, Gass M, Muller K, Skepper JN, Midgley PA, Welland M. 2007. Direct imaging of single-walled carbon nanotubes in cells. Nat Nanotechnol 2:713–717.

Ramirez P, Eastmond DA, Laclette JP, Ostrosky-Wegman P. 1997. Disruption of microtubule assembly and spindle formation as a mechanism for the induction of aneuploid cells by sodium arsenite and vanadium pentoxide. Mutat Res 386:291–298.

Risom L, Moller P, Loft S. 2005. Oxidative stress-induced DNA damage by particulate air pollution. Mutat Res 592:119–137.

Rubin H. 2001. Synergistic mechanisms in carcinogenesis by polycyclic aromatic hydrocarbons and by tobacco smoke: A bio-historical perspective with updates. Carcinogenesis 22:1903–1930.

Sakamoto Y, Nakae D, Fukumori N, Tayama K, Maekawa A, Imai K, Hirose A, Nishimura T, Ohashi N, Ogata A. 2009. Induction of mesothelioma by a single intrascrotal administration of multi-wall carbon nanotube in intact male Fischer 344 rats. J Toxicol Sci 34:65–76.

Salisbury JL. 2008. Breaking the ties that bind centriole numbers. Nat Cell Biol 10:255–257.

Salisbury JL, D'Assoro AB, Lingle WL. 2004. Centrosome amplification and the origin of chromosomal instability in breast cancer. J Mammary Gland Biol Neoplasia 9:275–283.

Shvedova AA, Kisin ER, Mercer R, Murray AR, Johnson VJ, Potapovich AI, Tyurina YY, Gorelik O, Arepalli S, Schwegler-Berry D, Hubbs AF, Antonini J, Evans DE, Ku BK, Ramsey D, Maynard A, Kagan VE, Castranova V, Baron P. 2005. Unusual inflammatory and fibrogenic pulmonary responses to single-walled carbon nanotubes in mice. Am J Physiol Lung Cell Mol Physiol 289:L698–L708.

Shvedova AA, Kisin E, Murray AR, Johnson VJ, Gorelik O, Arepalli S, Hubbs AF, Mercer RR, Keohavong P, Sussman N, Jin J, Yin J, Stone S, Chen BT, Deye G, Maynard A, Castranova V, Baron PA, Kagan VE. 2008. Inhalation vs. aspiration of single-walled carbon nanotubes in C57BL/6 mice: inflammation, fibrosis, oxidative stress, and mutagenesis. Am J Physiol Lung Cell Mol Physiol 295:L552–L565.

Stanton MF, Layard M, Tegeris A, Miller E, May M, Morgan E, Smith A. 1981. Relation of particle dimension to carcinogenicity in amphibole asbestoses and other fibrous minerals. J Natl Cancer Inst 67:965–975.

Takagi A, Hirose A, Nishimura T, Fukumori N, Ogata A, Ohashi N, Kitajima S, Kanno J. 2008. Induction of mesothelioma in p53+/− mouse by intraperitoneal application of multi-wall carbon nanotube. J Toxicol Sci 33:105–116.

Tam IY, Chung LP, Suen WS, Wang E, Wong MC, Ho KK, Lam WK, Chiu SW, Girard L, Minna JD, Gazdar AF, Wong MP. 2006. Distinct epidermal growth factor receptor and KRAS mutation patterns in non-small cell lung cancer patients with different tobacco exposure and clinicopathologic features. Clin Cancer Res 12:1647–1653.

Warheit DB, Laurence BR, Reed KL, Roach DH, Reynolds GA, Webb TR. 2004. Comparative pulmonary toxicity assessment of single-wall carbon nanotubes in rats. Toxicol Sci 77:117–125.

Wiktor AE, Van Dyke DL, Stupca PJ, Ketterling RP, Thorland EC, Shearer BM, Fink SR, Stockero KJ, Majorowicz JR, Dewald GW. 2006. Preclinical validation of fluorescence in situ hybridization assays for clinical practice. Genet Med 8:16–23.

Yurov YB, Iourov IY, Monakhov VV, Soloviev IV, Vostrikov VM, Vorsanova SG. 2005. The variation of aneuploidy frequency in the developing and adult human brain revealed by an interphase FISH study. J Histochem Cytochem 53:385–390.

Zanello LP, Zhao B, Hu H, Haddon RC. 2006. Bone cell proliferation on carbon nanotubes. Nano Lett 6:562–567.

Accepted by—
D. Sackett